INTERNATIONAL JOURNAL FOR NUMERICAL METHODS IN FLUIDS, VOL. 3, 543–565 (1983)

# A MULTI-VORTEX MODEL OF LEADING-EDGE VORTEX FLOWS

A. J. PEACE

*School of Mathematics and Physics, University of East Anglia, Norwich, England*

SUMMARY

A multi-vortex model of the vortex sheets shed from the sharp leading edges of slender wings is considered. The method, which is developed within the framework of slender-body theory, is designed to deal with those situations in which more than one centre of rotation is formed on the wing, for example on a slender wing with lengthwise camber or with a strake. Numerical results are presented, firstly for situations where comparison can be made with a vortex sheet model and secondly for cases, such as those described above, where a vortex sheet model is unable to describe the flow. Where comparison is available, agreement is good and in the cases where more than one vortex system is present interesting interactions are obtained.

KEY WORDS Low-aspect Ratio Wings Leading-edge Separation Vortex Shedding

## 1. INTRODUCTION

The flow past a wing of low aspect ratio, placed at incidence, separates from the highly swept leading edges to form free shear layers. These layers are formed from the outward flowing boundary layers on the upper and lower surfaces of the wing merging at the leading edges. The subsequent growth of the layers takes place under the influence of their own external velocity field in which the velocities on either side of the layer are equal in magnitude but different in direction. On a symmetrical wing the result of this primary separation is to form spiral vortex structures above each half of the wing.

The simplest model of this type of flow was due to Brown and Michael[1] who, considering conical planforms, assumed all the vorticity to be concentrated into an isolated vortex above each half of the wing. The extension of this model to plane wings with curved leading edges has been considered by Smith.[2]

The subsequent vortex sheet model of separated flow over delta wings developed by Smith[3] has been successfully applied to several conical flow problems. This model assumes that the vorticity in the primary vortex shed from the leading edge is concentrated into an infinite spiral sheet with the outer part represented explicitly in the numerical calculation and with the infinite inner part of the sheet replaced by an isolated line vortex. The boundary conditions are that the sheet is a stream surface which can sustain no pressure difference and that the total force on the isolated vortex and cut joining it to the free end of the sheet is zero. A Kutta condition is also satisfied at the leading edge where the solution would otherwise be singular.

The extension of the vortex sheet model to non-conical planforms was investigated by Clark[4] who used it for the cases of a flat wing with curved leading edges and a delta wing with lengthwise camber. He found that the numerical calculation was unable to deal with the

0271–2091/83/060543–23$02.30

*Received 11 November 1981*
*Revised 3 August 1982*

flow over the cambered wing when a second vortex system of opposite sign began to be shed underneath the wing as the effective local incidence changed sign. He concluded that the method as it stood could not provide an adequate representation of the two vortex systems. The present investigation was undertaken with a view to developing a method capable of resolving this difficulty. All the above methods, together with the present one, are set within the framework of slender-body theory, that is that changes occurring in the streamwise direction are slow compared to those taking place in transverse planes; upstream influence is neglected.

As has been indicated, a more adaptive method is needed to deal with those situations in which more than one vortex system forms on a wing due to leading-edge separation. The model developed here is one in which the vortex sheets are modelled by a distribution of inviscid line vortices, viscosity being neglected except as a cause of separation. In this multi-vortex model the inner part of the sheet is represented by a single isolated core vortex. Discrete vortices are shed sequentially at intervals along the leading edge and wrap around the core vortex, the subsequent positions of which, as one proceeds downstream, describe the roll-up of the outer part of the sheet. The Kutta condition, which requires that the velocity at the leading edge is finite, is satisfied exactly at all streamwise stations.

A multi-vortex model has been applied by Sacks *et al.*[5] to non-conical leading-edge separation but with the absence of any distinct representation of the central core, the importance of which was emphasized by Moore.[6]

There is a clear analogy between non-conical calculations which march in space and time dependent two-dimensional flows and the method of representing vortex sheets by arrays of point vortices, or other forms of discretization, has been used recently to obtain numerical predictions of a large variety of such flows (see Reference 7 for a survey). A more recent application of vortex shedding is that due to Longuet-Higgins[8] who investigates the oscillatory flow over sand ripples. In all these flows, unlike those described in the present work, the Kutta condition is only satisfied exactly at the instant of introduction of each new vortex. Otherwise, it is only satisfied in some mean sense and, by the nature of the calculation, cannot be satisfied exactly. Graham,[9] however, in his study of the oscillatory flow around sharp-edged cylinders, employs a discrete vortex model as in the present work but in addition represents the first part of the configuration, at the separation point, by a sheet element.

As the number of vortices which are fed into the spiral sheet increases, the turns of the vortex sheet near the core become closer together and chaotic breakdown caused by unwanted vortex interactions in neighbouring turns ensues.[6] Various methods of attempting to delay the onset of this instability have been employed. Fink and Soh,[10] for example, introduce a technique which redistributes the vorticity after each integration step so that the vortices are equally spaced. This technique ensures that the contribution from the logarithmic singularity, in calculating the induced velocity on the sheet, vanishes. However, it is questioned by Moore[11] to what extent this technique provides a solution of the equations of motion. Another stabilizing technique is to amalgamate sheet vortices with the core[6] whenever the angular separation of vortices, when viewed from the core, exceeds some pre-assigned critical value. This process places a new vortex at the centroid of the amalgamating pair with circulation equal to the sum of the pairs circulation. However, this method of amalgamation has been shown by Portnoy[12] to introduce an additional vortex impulse into the flow. Longuet-Higgins[8] uses a different amalgamation technique which conserves both momentum and total circulation. In the present calculations an amalgamation process is used which is smoother than that used by Moore,[6] with no respacing of the remaining vortices employed.

In Sections 2 to 4 below the mathematical description of the model which we adopt is discussed. This includes derivation of the equations of motion, treatment of the boundary conditions, the method of introducing new vortices into the flow and expressions for the pressure and load on the wing. The solution procedure is detailed in Section 5 with the results presented and discussed in Section 6; comparison is made with previous sheet model calculations[3,4] where possible.

## 2. MATHEMATICAL FORMULATION

We consider a wing with axes $O'xy'z'$ centred on the wing apex, forming a right-handed system, so that $O'x$ is aligned with the free stream, speed $U$. With reference to Figures 1 and 2(a) local axes are introduced in the cross-flow plane, and are related to the axes through $O'$ by

$$y = y', \qquad z = z' + h(x), \tag{1}$$

where $h(x)$ is the distance of the wing centre line below $O'x$. The local angle of incidence $\alpha$

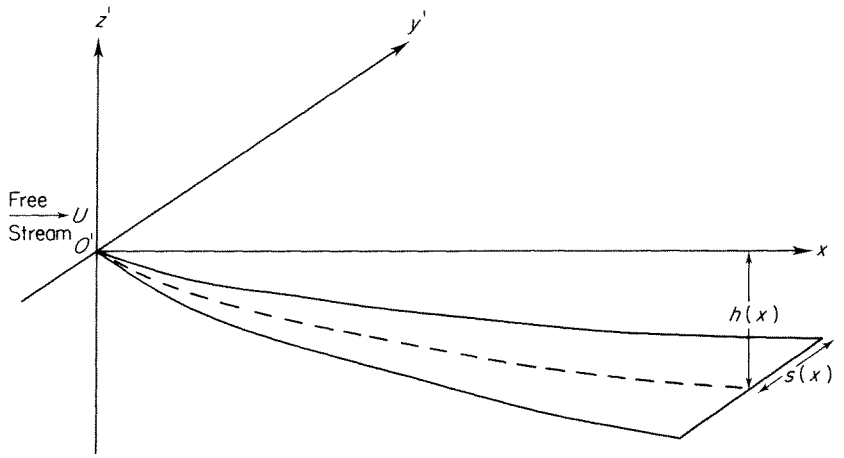


Figure 1. Typical wing and axis system

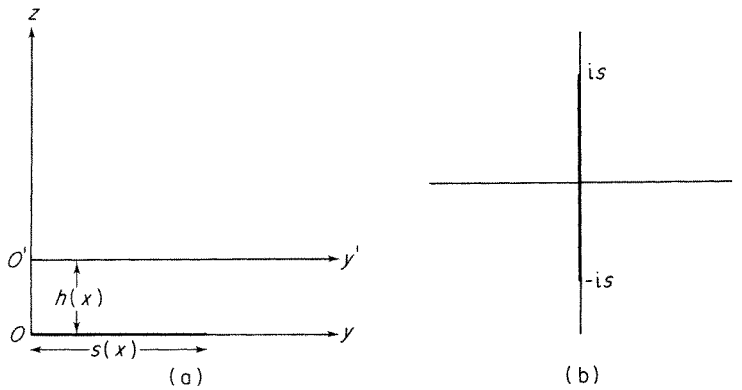


Figure 2. The co-ordinate systems: (a) the cross-flow plane; (b) the transformed plane

of the wing to the free stream which is assumed to be small, is therefore given by

$$\alpha(x) = h'(x). \tag{2}$$

The semi-span of the wing is denoted by $s(x)$.

If we write the velocity potential $\Phi$, with the velocity vector

$$\mathbf{v} = \nabla\Phi, \tag{3}$$

in the form

$$\Phi = Ux + \phi - Uzh'(x), \tag{4}$$

and apply the assumptions of slender-body theory,[13] the disturbance potential $\phi$ will satisfy the two-dimensional Laplace equation

$$\phi_{yy} + \phi_{zz} = 0 \tag{5}$$

in each cross-flow plane.[4] The problem then reduces to that of calculating the two-dimensional velocity field in each cross-flow plane; the three-dimensional nature of the problem enters only through the boundary conditions.

The boundary conditions are that the wing is a stream surface, so that

$$\phi_z = 0 \quad \text{on} \quad z = 0, \tag{6}$$

and that the disturbance decays at infinity to give

$$\phi \sim Uzh'(x) \tag{7}$$

at large distances from the wing. There is a mathematically acceptable attached-flow solution to the problem posed above but, for a real fluid, the flow will separate at the sharp leading edges resulting in the shedding of vortex sheets springing from these edges. The singularity in the attached flow solution is therefore physically unsatisfactory and its removal by viscosity is mathematically modelled by a Kutta condition of finite velocity at the leading edges.

The solution of the above is equivalent to seeking a complex analytic function $W(Z)$, where $Z = y + iz$ such that $\phi = \mathrm{Re}\{W\}$ satisfies all the boundary conditions.

We introduce a simplification of the problem by the mapping

$$Z^{*2} = Z^2 - s^2 \tag{8}$$

which transforms the $Z$-plane outside the slit representing the wing onto the $Z^*$-plane outside a slit lying on the imaginary axis, as in Figure 2(b). Since the imaginary axis represents the vertical plane of symmetry of the flow, the boundary condition (6) of zero velocity normal to the wing is now satisfied automatically in the $Z^*$-plane. At infinity $Z^* \sim Z$ so a function satisfying (7) is

$$W = -i\alpha UZ^* + f(Z^*), \tag{9}$$

where $|f(Z^*)| \sim o(1)$ as $|Z| \to \infty$, and $f(Z^*)$ is chosen to satisfy conditions associated with the vortex sheets including the Kutta condition.

We assume that the vortex sheets which spring from the leading edge can each be represented by a single line vortex, or core, which represents the concentrated inner spiral of the rolled-up vortex sheet, together with a number of line vortices which represent the outer part of the vortex sheet as in Figure 3. The strengths of these sheet vortices are constant except for the last shed vortex, which is assumed to absorb all the vorticity, from the point at

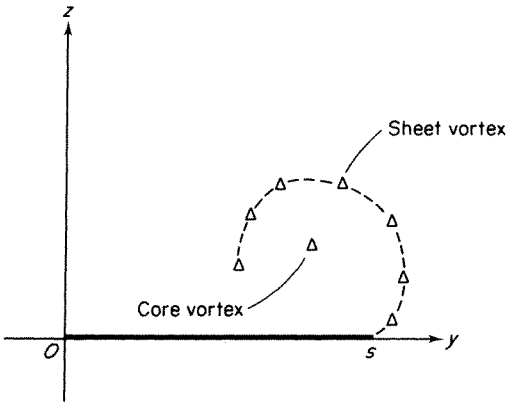


Figure 3. Typical vortex system in the cross-flow plane

which it leaves the leading edge, which would have been shed from the leading edge into the vortex sheet, and also vortices undergoing amalgamation in the manner described below.

If $n$ vortices are present to describe the vortex sheet which is shed from each leading edge, in a particular cross-flow plane, the complex potential in the transformed plane which both satisfies the boundary conditions, and incorporates the multi-vortex sheet description, is given by

$$W = -\mathrm{i}\alpha U Z^* + \sum_{i=1}^{n} \frac{\Gamma_i}{2\pi \mathrm{i}} \ln\left(\frac{Z^* - Z_i^*}{Z^* + \bar{Z}_i^*}\right), \tag{10}$$

where an overbar denotes the complex conjugate.

The complex conjugate velocities in the two planes are related, using (7), by

$$(v - \mathrm{i}w)_Z = \frac{\mathrm{d}W}{\mathrm{d}Z} = \frac{\mathrm{d}W}{\mathrm{d}Z^*}\frac{\mathrm{d}Z^*}{\mathrm{d}Z} = \frac{\mathrm{d}W}{\mathrm{d}Z^*}\frac{Z}{Z^*} = (v - \mathrm{i}w)_{Z^*} \cdot \frac{Z}{Z^*}, \tag{11}$$

where, in the $Z$-plane, $v = \phi_y$ and $w = \phi_z$ and from (10)

$$\frac{\mathrm{d}W}{\mathrm{d}Z^*} = -\mathrm{i}\alpha U + \sum_{i=1}^{n} \frac{\Gamma_i}{2\pi \mathrm{i}} \left(\frac{1}{Z^* - Z_i^*} - \frac{1}{Z^* + \bar{Z}_i^*}\right), \tag{12}$$

To satisfy the condition of finite velocity at the leading edges, $Z = \pm s$, the Kutta condition requires that, from (11),

$$\frac{\mathrm{d}W}{\mathrm{d}Z^*} = 0 \quad \text{at} \quad Z^* = 0. \tag{13}$$

From (12) this may be written as

$$2\pi\alpha U = \sum_{i=1}^{n} \Gamma_i \frac{(Z_i^* + \bar{Z}_i^*)}{Z_i^* \bar{Z}_i^*}. \tag{14}$$

The position of a line vortex of constant strength at $Z = Z_i$, which must align itself with the local flow direction, is given by

$$U\frac{\mathrm{d}\bar{Z}_i}{\mathrm{d}x} = \lim_{Z \to Z_i} \frac{\mathrm{d}W'}{\mathrm{d}Z}. \tag{15}$$

where

$$W' = W - \frac{\Gamma_i}{2\pi \mathrm{i}} \ln (Z - Z_i). \tag{16}$$

Using (10), (15) becomes

$$\frac{\mathrm{d}\bar{Z}_i}{\mathrm{d}x} = \frac{Z_i}{2\pi i U Z_i^*} \left\{ 2\pi\alpha U + \sum_{\substack{j=1 \\ j\neq i}}^{n} \frac{\Gamma_j (Z_j^* + \bar{Z}_j^*)}{(Z_i^* - Z_j^*)(Z_i^* + \bar{Z}_j^*)} - \frac{\Gamma_i}{Z_i^* + \bar{Z}_i^*} - \frac{\Gamma_i s^2}{2 Z_i^2 Z_i^*} \right\}; \qquad i = 1, \ldots, n-1. \tag{17}$$

The last shed vortex (subscript $n$) whose strength is changing must be attached to the leading edge by a cut to ensure that flow variables are single valued. This cut can be thought of as a surface which carries transverse vorticity from the leading edge into the vortex. Equation (15), which implies that the vortex is force-free, is now replaced by a condition which ensures that the total force on the vortex and cut is zero. The pressure jump across the cut gives rise to a force

$$\mathrm{i}\rho U (Z_n - s) \frac{\mathrm{d}\Gamma_n}{\mathrm{d}x}, \tag{18}$$

where products in the disturbance velocities have been neglected, and $\rho$ is the density. The force on the vortex itself is given by

$$-\mathrm{i}\rho\Gamma_n \left( \lim_{Z \to Z_n} \frac{\mathrm{d}\bar{W}'}{\mathrm{d}Z} - U \frac{\mathrm{d}Z_n}{\mathrm{d}x} \right). \tag{19}$$

The condition of zero total force on the combination of vortex and cut may then be written as

$$\Gamma_n \frac{\mathrm{d}\bar{Z}_n}{\mathrm{d}x} + (\bar{Z}_n - s) \frac{\mathrm{d}\Gamma_n}{\mathrm{d}x} = \frac{\Gamma_n}{U} \lim_{Z \to Z_n} \frac{\mathrm{d}W'}{\mathrm{d}Z}. \tag{20a}$$

The stability of a multi-vortex model of this type, that is, one in which a core is identified, is enhanced if vortices at the free end of the sheet are amalgamated with the core vortex when the sheet is assumed to be adequately described, in the sense described in Section 5. This amalgamation process takes the form of introducing a cut, as before, but now between the core vortex, subscript 1, and the last sheet vortex, subscript 2, and again satisfying a zero total force condition on the core vortex and cut as the vorticity is transferred. Thus

$$\Gamma_1 \frac{\mathrm{d}\bar{Z}_1}{\mathrm{d}x} + (\bar{Z}_1 - \bar{Z}_2) \frac{\mathrm{d}\Gamma_1}{\mathrm{d}x} = \frac{\Gamma_1}{U} \lim_{Z \to Z_1} \frac{\mathrm{d}W'}{\mathrm{d}Z}. \tag{20b}$$

This equation will then replace equation (17) with $i = 1$.

We have described above a model of the vortex sheet, which forms at the leading edge of a slender wing, in which vorticity is created at the leading edge in the form of a succession of line vortices growing from it. These vortices spiral around a central vortex core, which itself represents the tightly wound inner vortex sheet, and are amalgamated with it when the outer part of the sheet is deemed to be adequately represented as measured, for example, by its angular extent. The novel feature of the present treatment is that the circulation of each line vortex varies continuously with the streamwise distance $x$. On the one hand this should provide a better approximation to the continuous development of the flow, and, on the

other, it should reduce the magnitude of disturbances, so that the onset of instability is delayed.

## 3. VORTEX INTRODUCTION

Equations (14), (17) and (20) are sufficient to determine $Z_i$; $i = 1, \ldots, n$, and $\Gamma_n$ as functions of the streamwise variable $x$. However, there are difficulties in starting a numerical integration at a point where a new vortex is about to be introduced into the flow at, say, $x = x_0$ due to the rapid changes in the circulation of the new vortex. To overcome this, Smith[14] has developed a solution of the equations of motion in powers of $x$ from which initial values for a numerical integration at $x = x_0 + \varepsilon$ $(\varepsilon > 0)$ may be obtained. A brief account of these expansions are given below, for a more detailed derivation see Peace—Reference 15.

Without loss of generality we can assume $x_0 = 0$ and then the wing can be described as that portion of the plane $z = 0$ for which $|y| \leqslant s(x)$ where

$$K = \left.\frac{\mathrm{d}s}{\mathrm{d}x}\right|_{x=0+} \tag{21}$$

and a discontinuity in $K$ is permitted at $x = 0$. Writing

$$\left.\begin{aligned} Z_i(x) &= Z_i(0) + xZ_i'(0) + O(x^2); \qquad x \geqslant 0 \\ \Gamma_n \frac{(Z_n^* + \bar{Z}_n^*)}{Z_n^* \bar{Z}_n^*} &= \frac{2\pi A U x}{s_0} + O(x^2) \\ \frac{(v - \mathrm{i}w)_Z}{U} &= B + \mathrm{i}C\frac{Z^*}{s_0} + O\left(\frac{Z^{*2}}{s_0^2}\right) \\ Z_n^* &= s_0(\sigma + \mathrm{i}\tau) \\ \xi &= x/s_0 \end{aligned}\right\} \tag{22}$$

where $s_0 = s(0)$, the following composite expansions are obtained from (14), (17) and (20).

(i) $K \geqslant B$

$$\left.\begin{aligned} \sigma &= \frac{\xi^{5/6}}{\left(\frac{2(K-B)}{3}\right)^{1/2}\left(\frac{6}{A}\right)^{2/3} + \left(\frac{12}{A}\right)^{1/3}\xi^{1/6}} \\ \tau &= \frac{\xi + 2^{1/3}(K-B)}{\xi + (K-B)}\left(\frac{A}{12}\right)^{1/3}\xi^{2/3} \\ \frac{\Gamma_n}{2\pi U s_0} &= A\left(\frac{K-B}{6}\right)^{1/2}\xi^{3/2} + A\left|\frac{A}{12}\right|\xi^{5/3} \end{aligned}\right\} \tag{23}$$

(ii) $K < B$

$$\left.\begin{aligned} \sigma &= \left(\frac{4(B-K)}{5}\right)^{1/2}\xi^{1/2} + \left|\frac{A}{12}\right|^{1/3}\xi^{2/3} \\ \tau &= \frac{\xi}{\frac{24(B-K)}{5A - 8C(B-K)} + \left(\frac{12}{A}\right)^{1/3}\xi^{1/3}} \\ \frac{\Gamma_n}{2\pi U s_0} &= A\left(\frac{B-K}{5}\right)^{1/2}\xi^{3/2} + A\left|\frac{A}{12}\right|^{1/3}\xi^{5/3} \end{aligned}\right\} \tag{24}$$

where

$$\left.\begin{aligned} A &= \frac{s_0}{2\pi}\left\{2\pi\alpha' + \sum_{i=1}^{n-1}\frac{\Gamma_i}{U}\left(\frac{Z_i}{Z_i^{*3}}Z_i'(0) - \frac{Ks_0}{Z_i^{*3}} + \frac{\bar{Z}_i}{\bar{Z}_i^{*3}}\bar{Z}_i'(0) - \frac{Ks_0}{\bar{Z}_i^{*3}}\right)\right\} \\ B &= \frac{s_0}{2\pi i U}\sum_{i=1}^{n-1}\Gamma_i\frac{(Z_i^{*2} - \bar{Z}_i^{*2})}{Z_i^{*2}\bar{Z}_i^{*2}} \\ C &= \frac{s_0^2}{2\pi U}\sum_{i=1}^{n-1}\Gamma_i\frac{(Z_i^{*3} + \bar{Z}_i^{*3})}{Z_i^{*3}\bar{Z}_i^{*3}} \end{aligned}\right\} \tag{25}$$

and a prime denotes differentiation with respect to $x$. The local flow velocity at $x_0$ from the third of equations (22) results in a different asymptotic behaviour depending upon whether the local flow direction immediately downstream of $x_0$ is outboard ($B > K$) or inboard ($B < K$) of the leading edge. Hence the first of equations (22) together with (23) or (24) furnish us with a starting solution for the numerical integrations of (17) and (20) during the shedding of each vortex; equation (14) is satisfied throughout.

## 4. PRESSURE AND LIFT

The local normal force coefficient on the wing, $c_N(x)$, can be obtained by direct numerical integration of the pressure jump $\Delta C_p$ across the wing, where the operator $\Delta$ denotes lower surface minus upper surface. Thus

$$c_N(x) = \frac{1}{s}\int_0^s \Delta C_p \, dy, \tag{26}$$

where $C_p$ is defined and calculated in the usual manner according to slender-body theory.[3] The overall normal force coefficient is then

$$\begin{aligned} C_N &= \frac{2}{S}\int_0^l \int_0^s \Delta C_p \, dy \, dx \\ &= \frac{2}{S}\int_0^l s(x) c_N(x) \, dx, \end{aligned} \tag{27}$$

where $l$ is the length of the wing and $S$ is its area. For a conical flow, $c_N$ is constant and $C_N = c_N$.

Alternatively, the overall lift can be obtained from a momentum argument[13] so that, using (8) and (10),

$$C_N = \frac{1}{S}\left\{2\pi\alpha s^2 + 2\sum_{i=1}^{n}\frac{\Gamma_i}{U}\left\{Z_i^* + \bar{Z}_i^*\right\}\right\}, \tag{28}$$

and, from (27),

$$c_N(x) = \frac{1}{s}\frac{d}{dx}\left\{\pi\alpha s^2 + \sum_{i=1}^{n}\frac{\Gamma_i}{U}(Z_i^* + \bar{Z}_i^*)\right\}, \tag{29}$$

## 5. SOLUTION PROCEDURE

The problem is to determine the $2n$ unknown vortex co-ordinates $y_i$, $z_i$ ($Z_i = y_i + iz_i$); $i = 1, \ldots, n$ and the unknown vortex strength $\Gamma_n$, which gives $2n+1$ unknowns in all.

Elimination of $\Gamma_n$ using (14) leaves $2n$ unknowns and in (17); $i = 1, \ldots, n-1$ and (20a) we have $2n$ equations or, if amalgamation is taking place and so $d\Gamma_1/dx$ is specified (see below), we have $2n-4$ equations from (17); $i = 2, \ldots, n-1$ and 4 equations from (20a) and (20b) to give, again, a total of $2n$ equations.

Hence, the problem is reduced to solving a system of coupled, first order, ordinary differential equations of the form

$$\frac{d\eta_i}{dx} = f_i(x, \eta_1, \ldots, \eta_{2n}); \qquad i = 1, \ldots, 2n, \tag{30a}$$

where $\eta_i$ stands for an unknown vortex co-ordinate, i.e. $y_i$, $z_i$; $i = 1, \ldots, n$. The initial conditions are obtained from Section 3 and can be written as

$$\eta_i(x_0 + \varepsilon) = \eta_{i0}; \qquad i = 1, \ldots, 2n. \tag{30b}$$

The initial-value problem (30) is solved by integrating stepwise in the $x$-direction, during the growth of each vortex, using a variation of a fourth order Runge–Kutta method due to Merson.[16] The method evaluates the local truncation errors at each station using only data from the previous upstream solution. This enables the truncation errors to be monitored and kept within some prescribed tolerance by varying the size of the integration step length if necessary.

The scheme which is employed starts each calculation with a single vortex representation[1] of the vortex system over some part of the initial conical planform at the wing apex. Thereafter vortices are shed sequentially from the leading edge: their motion is calculated by the method described above, with the streamwise distance $x_s$ (the shedding length) over which a vortex is shed maintained at some constant value throughout the calculation. Only the last shed vortex, and vortices undergoing amalgamation, are changing in strength; the other vortices remain of constant strength. When the vortices have wrapped around the core to the extent that a prescribed sheet length is achieved, the one at the end of the sheet is amalgamated with the core vortex. This amalgamation process takes place over the same shedding length, $x_s$, and the rate of transfer of vorticity is prescribed as a linear function of $x$ so that, in (20b), $d\Gamma_1/dx = \Gamma_2/x_s$. The values of $\Gamma_1$ and $\Gamma_2$ are updated after each integration step during the shedding length.

Difficulties arise during the course of the calculation discussed above when the sign of the vorticity shed from the leading edge changes. The difficulty takes the form of an insistence by the method that it requires smaller and smaller integration steps, as $\Gamma_n \to 0$, to keep the truncation errors within the prescribed tolerance and so makes the calculation impractically long. To overcome this, a variation on the above method was introduced which considers the flow to be attached during this 'transition' period; that is, $\Gamma_n$ is set to zero and vorticity is no longer shed from the leading edge. The Kutta condition is therefore then only approximately satisfied.

This transition period is monitored using the parameter $A$ of the second of equations (22) which is small when the shed vorticity is small. If we define a small critical value of $A$, $A_{crit}$, we require that vorticity shall not be shed when $|A| \leqslant A_{crit}$; shedding is recommenced when $|A| > A_{crit}$ and the Kutta condition is reintroduced.

In situations when a second centre of rotation is obviously about to form, for example on the delta wing with lengthwise camber discussed in the next section, the vortex which signifies its genesis is grown for a number of normal shedding lengths, usually between 5 and 10, to provide a substantial centre of rotation which subsequent vortices can encircle to

represent the sheet in this new position. This process is essentially the counterpart of the original single vortex representation[1] which commences the solution at the wing apex.

## 6. RESULTS AND DISCUSSION

The method described in Section 5 has been applied to a number of wings; the results of the calculations are given below. The first example is primarily intended as a check on the method from a comparison of the results obtained from the vortex-sheet model for a delta wing.[3] A further comparison with a wing of gothic planform is made in Reference 15. The second example of the wing with chordwise camber continues the flow description past the point at which the vortex-sheet calculation[4] breaks down; again a comparison can be made up to that point. The third and fourth examples exploit the method to describe the flow over other wings of interest.

(i) *Flat delta wing*

The wing chosen is defined by

$$s(x) = 0{\cdot}2x, \qquad x \geqslant 0$$
$$h(x) = 0{\cdot}2x, \qquad x \geqslant 0$$

so that the leading edges are straight and the incidence is constant. Although the flat delta wing is conical in planform throughout, the calculation is here treated as an essentially non-conical one, in that the solution is computed at each streamwise station as we march downstream in the manner described in the preceding section. The incidence parameter[3] associated with the wing is $a = \tan\alpha/K = 1{\cdot}0$ where $K = \tan\gamma$ and $\gamma$ is the semi-apex angle. The vortex-sheet results[3] exploit the conicality of the wing and so define a similarity solution such that the solution at any streamwise station is obtained from a single scaled solution. The total circulation, in its similarity from $\Gamma/KUs$, is thus constant at all cross-sections, as in the sheet shape when lengths are scaled with the semi-span, $s$.

In order to investigate the asymptotic nature of the multi-vortex model as $x \to \infty$ the solution was continued downstream until the total circulation, scaled with the wing semi-span, remained constant. In such a calculation a constant shedding length results in an unreasonably large number of vortices describing the sheet, with correspondingly large computation times. To overcome this a conical shedding length was introduced with $x_s = ks$ where $k$ can be chosen to vary the number of vortices which represent the sheet. The results for total circulation, for increasing vortex 'densities' in the sheet, are shown in Figure 4; all

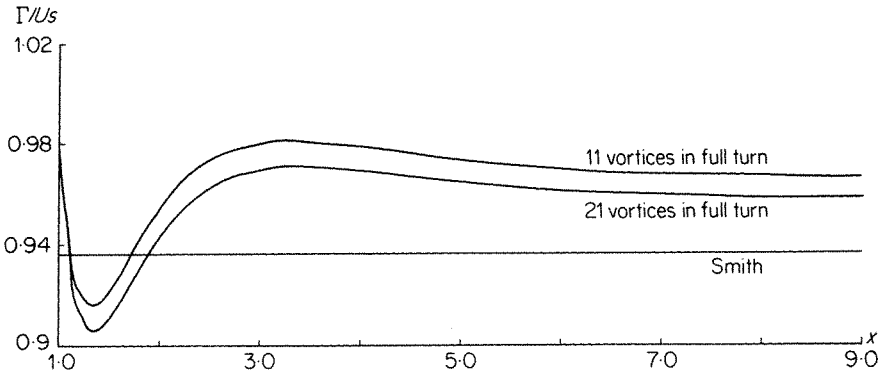


Figure 4. Flat delta wing—total circulation

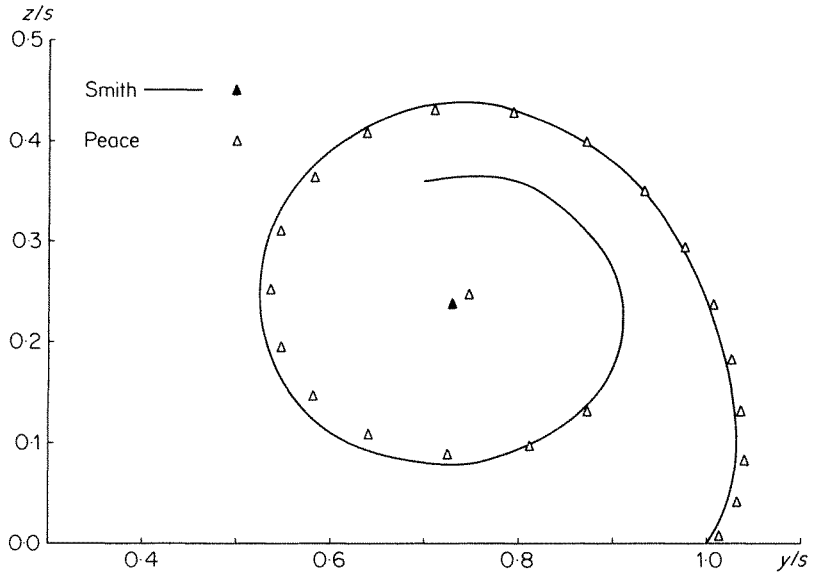


Figure 5. Flat delta wing—vortex sheet shape

sheets are of one full turn in extent. For the most dense case, the vortex sheet shape and wing pressure distribution are plotted in Figures 5 and 6.

As can be seen, increasing the density of vortices in the sheet increases the closeness of the value of total circulation as calculated by the present method to that calculated by Smith.[3] The sheet shape, which is plotted when the total circulation has reached an almost constant

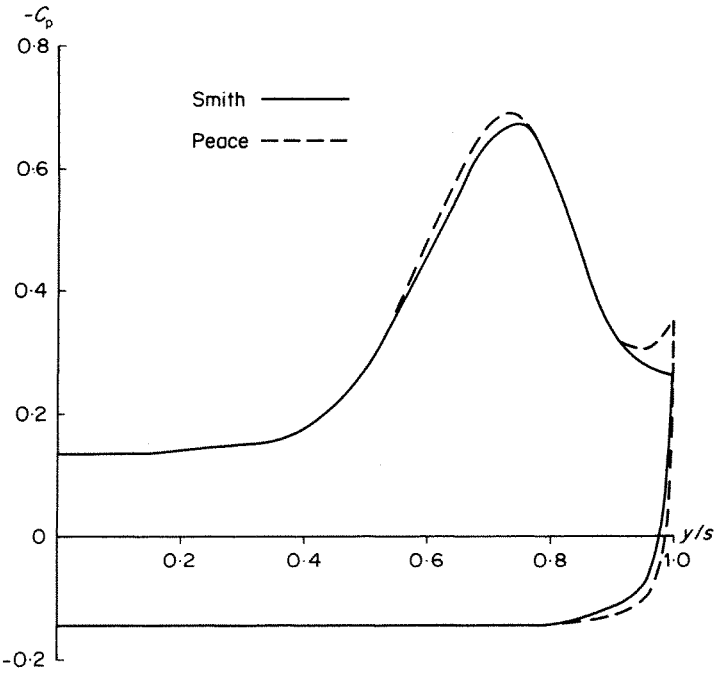


Figure 6. Flat delta wing—pressure distribution

value at $x = 9{\cdot}94$, is virtually coincident with Smith's result, with only a slight variation in the core position. Again it may be noted that quite good agreement is still achieved upstream of this position. However, the pressure distribution does show some differences. First, the present results show a higher suction peak than Smith's and secondly the present results show a larger pressure difference near the leading edge. The first discrepancy is probably due to the fact that more vorticity is concentrated in the core vortex in the present results and the second, in a sense, is to be expected since it is generally accepted that a multi-vortex model is less able to accurately describe a vortex sheet close to the separation point than at other points of the sheet. In fact, as was mentioned earlier, some vortex models[9] represent the first increment of the vortex sheet by an actual sheet element. The local normal force coefficient was calculated from both equations (26) and (29), and agreement to three significant figures was obtained between the two, with a value of 0·455. This may be compared with the value 0·443 given by Smith.[3]

There is, of course, a certain degree of arbitrariness in the point chosen in the shedding cycle at which one analyses results. To show the kind of behaviour which occurs within the shedding cycle, Figures 7(a) and (b) show the variation of total circulation ($\Gamma/Us$) for separate cycles at two different positions in the above calculation for the most dense vortex sheet. The positions shown are (a) at the point where a complete turn of the sheet has just

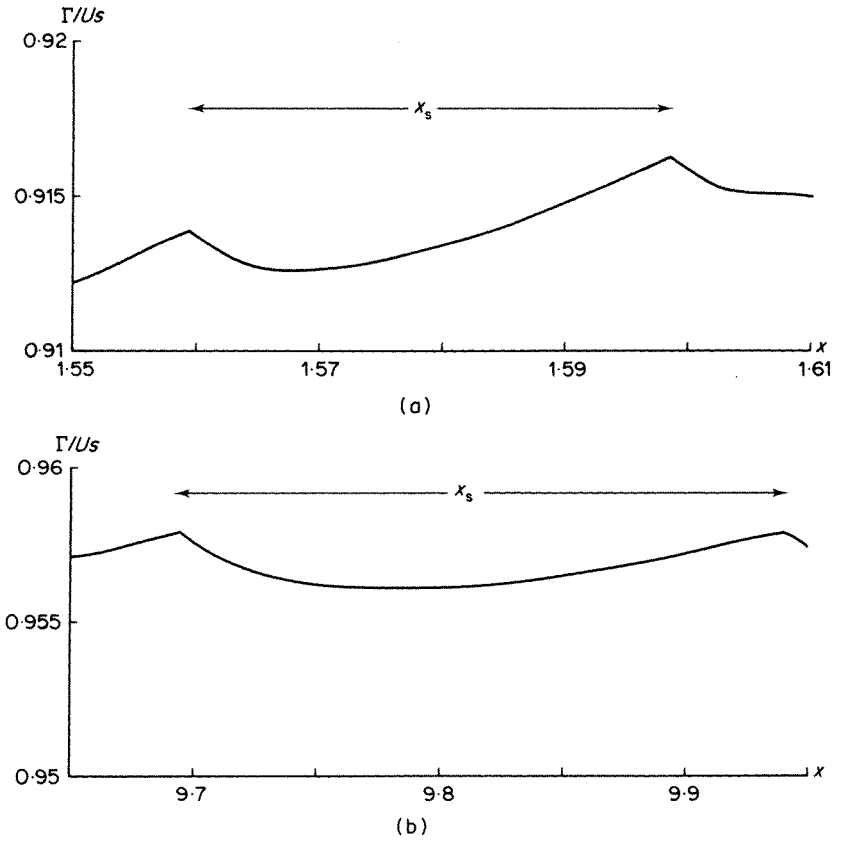


Figure 7. Variation in total circulation during shedding cycle for delta wing: (a) full turn of sheet just achieved; (b) total circulation reached constant value

been achieved ($x = 1{\cdot}56$) and (b) at the point where the total circulation, when sampled solely at the end of each shedding cycle, has achieved an almost constant value ($x = 9{\cdot}7$). The maximum variation within the shedding cycle is 0·4 per cent in the first case and 0·2 per cent in the second.

For all the results presented here, the vortex sheet shapes and values of total circulation are sampled at the end of the shedding cycle. However, the pressure and normal force coefficients are evaluated at the midpoint of the shedding cycle since the rate of change of total circulation is discontinuous at the end points, as can be seen from Figure 7. The pressures and normal force are thus discontinuous at these points. One could choose other positions in the cycle so as to make the results, e.g. pressure distribution, apparently agree more favourably but such a choice would have no mathematical basis. It may also be noted here that, with reference to Figure 7, most other multi-vortex models produce a discontinuity in the variation of total circulation with $x$ (or time) at the point of introduction of each new vortex.

(ii) *Delta wing with lengthwise camber*

Results have been obtained for the wing defined by

$$s(x) = 0{\cdot}25x, \qquad x \geqslant 0$$
$$h(x) = \begin{cases} 0{\cdot}2x, & 0 \leqslant x \leqslant 1 \\ 0{\cdot}1(4x - x^2 - 1), & x > 1 \end{cases}$$

which corresponds to a wing which is initially conical, as far as $x = 1$, with an angle of

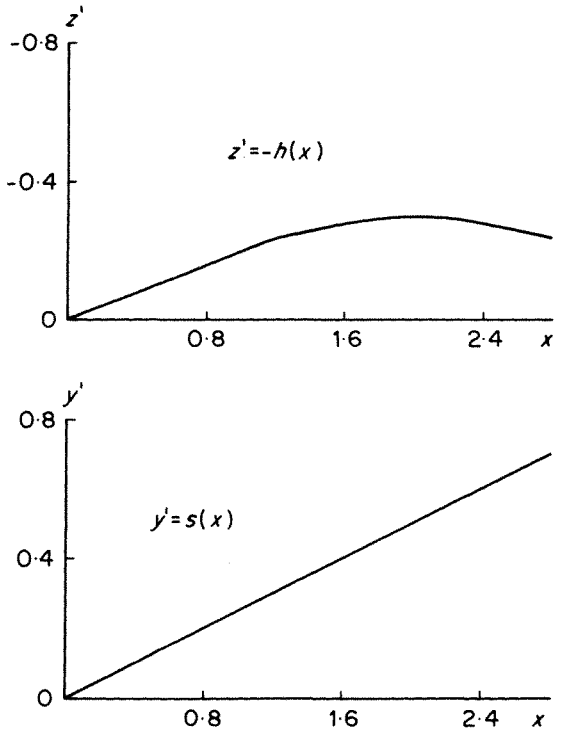


Figure 8. Cambered wing—planform and centre-line

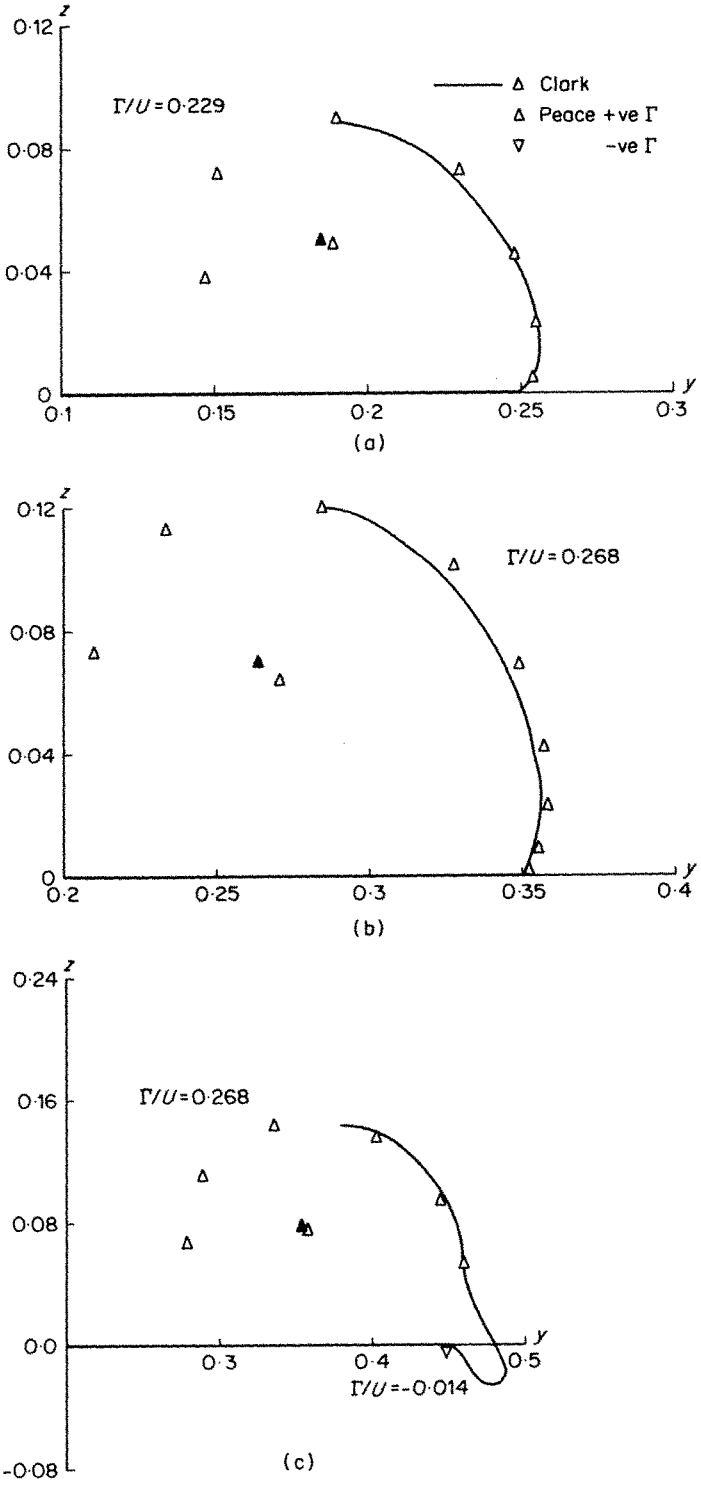


Figure 9. Cambered wing—sheet shapes: (a) $x = 1{\cdot}0$; (b) $x = 1{\cdot}4$; (c) $x = 1{\cdot}8$

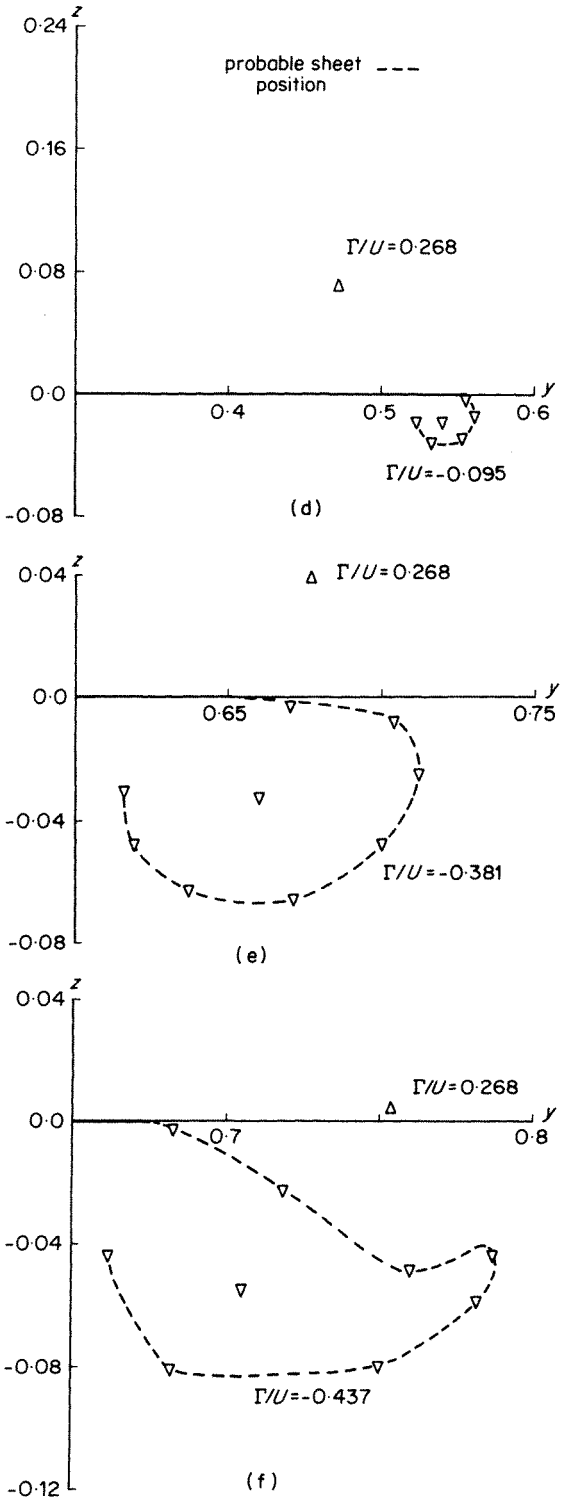


Figure 9. (*Continued*). Cambered wing—sheet shapes: (d) $x = 2{\cdot}2$; (e) $x = 2{\cdot}6$; (f) $x = 2{\cdot}7$

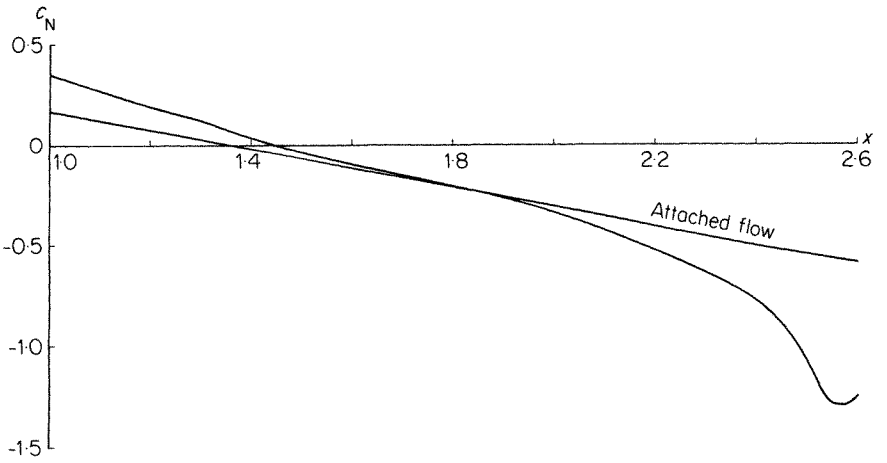


Figure 10. Cambered wing—local normal force coefficient

incidence of about 0·2 radians, downstream from which the local angle of incidence decreases linearly, reaching zero at $x = 2$ as shown in Figure 8. Comparison is made with Clark's results,[4] up to the point where his calculation fails, in Figures 9(a) to (c). The calculation fails because his method is unable to describe the vortex sheet shape as a second centre of rotation of opposite sign forms beneath the wing. The present method allows the calculation to continue downstream from this point, and the development of the second vortex system is shown in Figures 9(d) to (f); the total circulation of each system is shown separately. The broken line between the sheet vortices shows the probable position of the vortex sheet. The upper vortex system, which, owing to continued amalgamation, has reduced to a single vortex representation by $x = 2{\cdot}2$ is eventually convected outboard along the wing and moves into the region occupied by the lower vortex system. This interaction of the two systems results in a warping of the vortex sheet and eventually chaotic motion of the vortex sheet elements as the two systems merge together and sweep each other away from the leading edge. At this point it may be that a wholly inviscid approach is no longer adequate. The variation of the local normal force coefficient as one proceeds downstream is shown in Figure 10 together with the attached flow solution. The coefficients are constant in the conical section, $0 \leq x \leq 1$. As can be seen, additional force is generated from the presence of the vortex system on the forward part of the wing and as the second vortex system grows beneath the wing the force coefficient decreases and reduces below the attached flow solution. As the systems are swept off the wing an increase in force coefficient is observed.

(iii) *Double-delta wing*

This wing, shown in Figure 11, consists of an initial conical section attached to a truncated delta wing with a larger semi-apex angle so that the semi-span is continuous but the leading-edge slope is not. The semi-span is thus defined as

$$s(x) = \begin{cases} 0{\cdot}1x, & 0 \leq x \leq 10 \\ 1{\cdot}0 + 0{\cdot}4(x-10), & x > 10. \end{cases}$$

The wing models a type of straked wing for which one vortex system forms on the initial

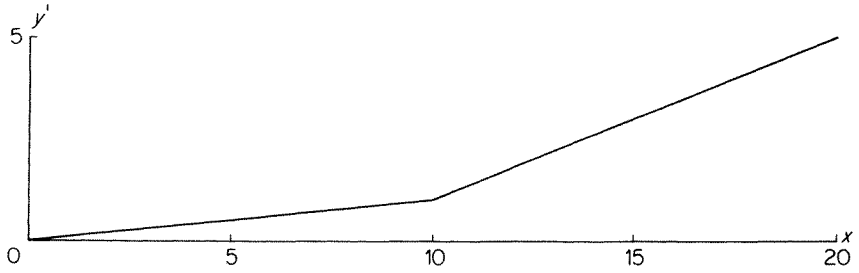


Figure 11. Double-delta wing planform

conical part of the wing, and a second system begins at the discontinuity and stays in the vicinity of the leading edge. The main interest lies in whether (a) the first system maintains its own identity and follows a path along some inboard portion of the wing, or (b) the first system is eventually drawn towards the second and merges with it. The angle of incidence obviously affects which of these situations will occur and to investigate this Fiddes[17] has performed calculations in which each vortex system is represented by a single vortex. On increasing the incidence gradually he found that the first value at which type (b) behaviour is encountered, within the distance his calculations proceeded downstream, is $\alpha = 0{\cdot}18$. This incidence is also used in our calculation together with a smaller incidence of $\alpha = 0{\cdot}1$ which does indeed produce type (a) behaviour. The two sets of results are described below.

(a) $\alpha = 0{\cdot}1$. In Figures 12(a) to (e) we show the sheet shapes at various streamwise stations. The two configurations are seen to be moving outboard and becoming further apart as they proceed downstream. The last shed vortex of the first configuration can be seen to be 'undecided' as to which configuration to 'join' and, although here it moves towards the first, calculations have been performed for a slightly larger incidence where it is captured by the second system.

(b) $\alpha = 0{\cdot}18$. Sheet shapes for this incidence are shown in Figures 13(a) to (f). As can be seen, the first configuration is drawn outboard by its image vorticity in the wing towards the second and is eventually swept beneath it. Before the configurations merge, instability occurs in the outboard configuration, not at the point of first 'contact', as one might have expected, but on the straightest portion of the sheet springing from the leading edge. This may be due to the classical Helmholtz instability, which is inhibited in the curved part of the vortex sheet due to its rapid stretching. This explanation was put forward in a similar case by Moore[6] in his calculations and later theoretically justified by him.[18] Once instability has commenced it is convected around the sheet and, again, as the systems merge, and also as the first moves very close to the wing, we may conjecture that a wholly inviscid approach cannot correctly model the situation.

(iv) *Lenticular wing*

This flat wing, which consists of a conical section whose edges join smoothly onto circular arcs, shown in Figure 14, is different from all the previous planforms in that the semi-span reaches a maximum value approximately half way down the wing and then recedes, so that the edges of the rear part of the wing are in fact trailing edges. Formally

$$s(x) = \begin{cases} 0{\cdot}25x, & 0 \leqslant x \leqslant 1{\cdot}0 \\ [17-(x-2)^2]^{1/2} - 3{\cdot}75, & 1{\cdot}0 < x < 3{\cdot}7139. \end{cases}$$

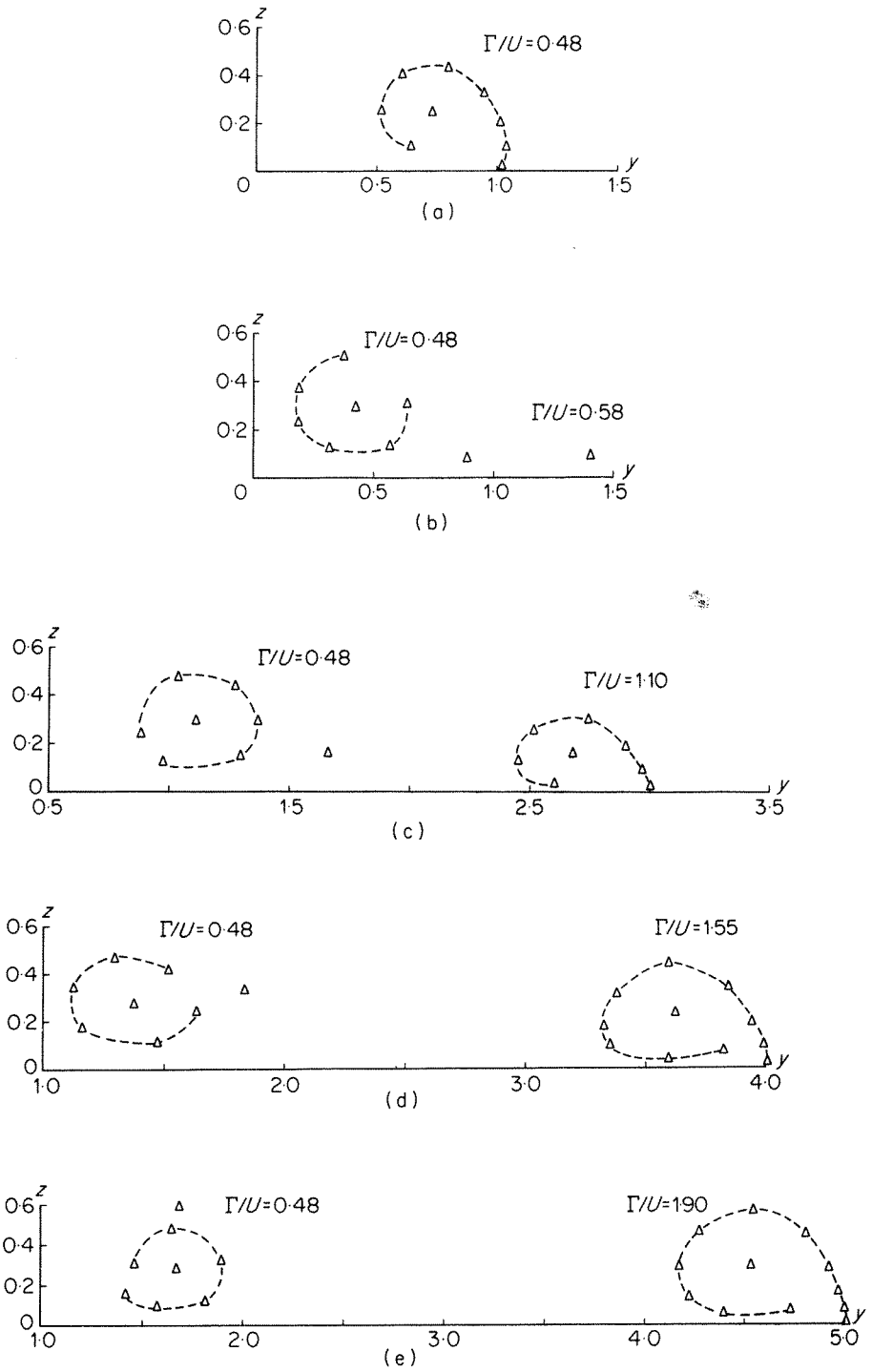


Figure 12. Double-delta wing—sheet shapes, $\alpha = 0{\cdot}1$: (a) $x = 10{\cdot}0$; (b) $x = 12{\cdot}5$; (c). $x = 15{\cdot}0$; (d) $x = 17{\cdot}5$; (e) $x = 20{\cdot}0$

The motivation for studying this wing came from the uncertainty as to whether or not a second vortex system might be formed beneath the wing as, when the wing recedes, the possibility arises that the downwash at the leading edge may be sufficient to cause such behaviour. Although this did not turn out to be the case, the three cases considered below show three distinct types of behaviour in the vorticity shed from the wing edges. Results for the sheet shapes, at the station $x = 3{\cdot}0$ near the rear of the wing, are shown in Figures 15(a) to (c).

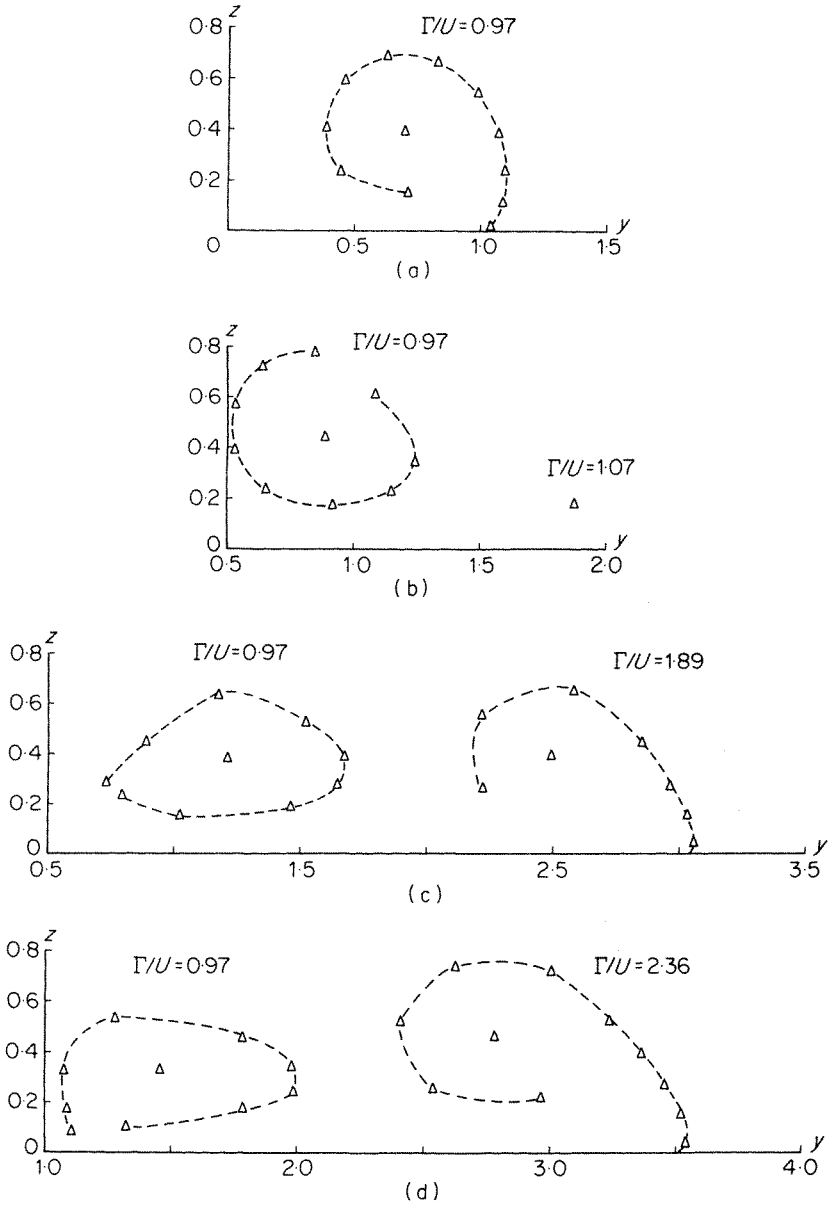


Figure 13. Double-delta wing—sheet shapes, $\alpha = 0{\cdot}18$: (a) $x = 10{\cdot}0$; (b) $x = 12{\cdot}5$; (c) $x = 15{\cdot}1$; (d) $x = 16{\cdot}3$

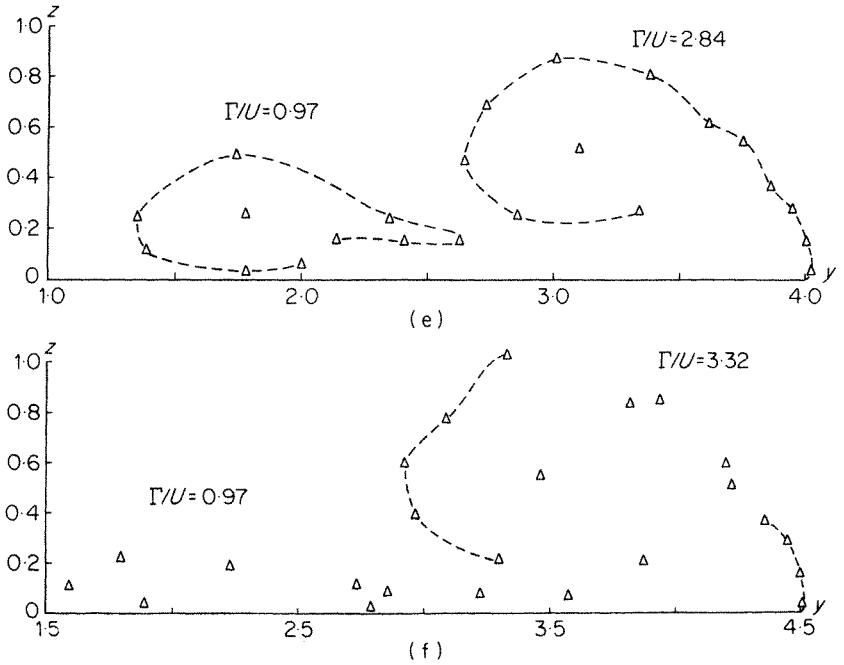


Figure 13. (*Continued*). Double-delta wing—sheet shapes, $\alpha = 0{\cdot}18$: (e) $x = 17{\cdot}5$; (f) $x = 18{\cdot}7$

(a) $\alpha = 0{\cdot}25$. Positive vorticity is shed down the whole length of the wing and rolls up into a vortex system which sits outboard of the wing edge as the semi-span reduces.

(b) $\alpha = 0{\cdot}2$. Positive vorticity is shed as far as $x = 2{\cdot}2$ with the strength of the shed vortices decreasing. At this station, with reference to the attached flow method described in Section 5, the parameter $A$ becomes less than the value of $A_{crit}$ set for the calculation. From there on $A$ reduces in size and then oscillates around $A = 0$ but with decreasing amplitude; it never moves outside the bounds set by $A_{crit}$. Hence no vorticity is shed after $x = 2{\cdot}2$. Obviously, decreasing the value of $A_{crit}$ would allow more vorticity to be shed but the strength of the shed vortices would be very small. In fact, we are, rather arbitrarily, saying that vortices of a certain size (in this case less than one hundredth of the core size) should be ignored.

(c) $\alpha = 0{\cdot}1$. In this example the shed vorticity changes sign and convects around the vortex sheet. However, at $x = 2{\cdot}8$ we reach a situation identical to that described in (b) above and no more vorticity is deemed to be shed in the calculation.

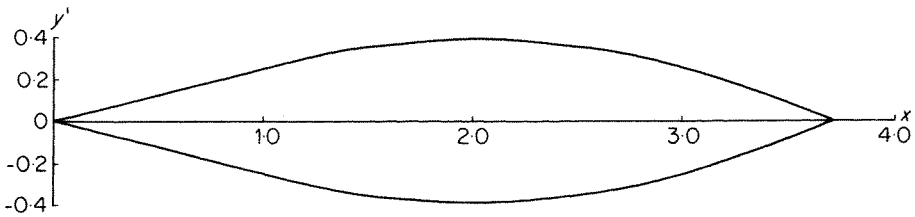

Figure 14. Lenticular wing planform

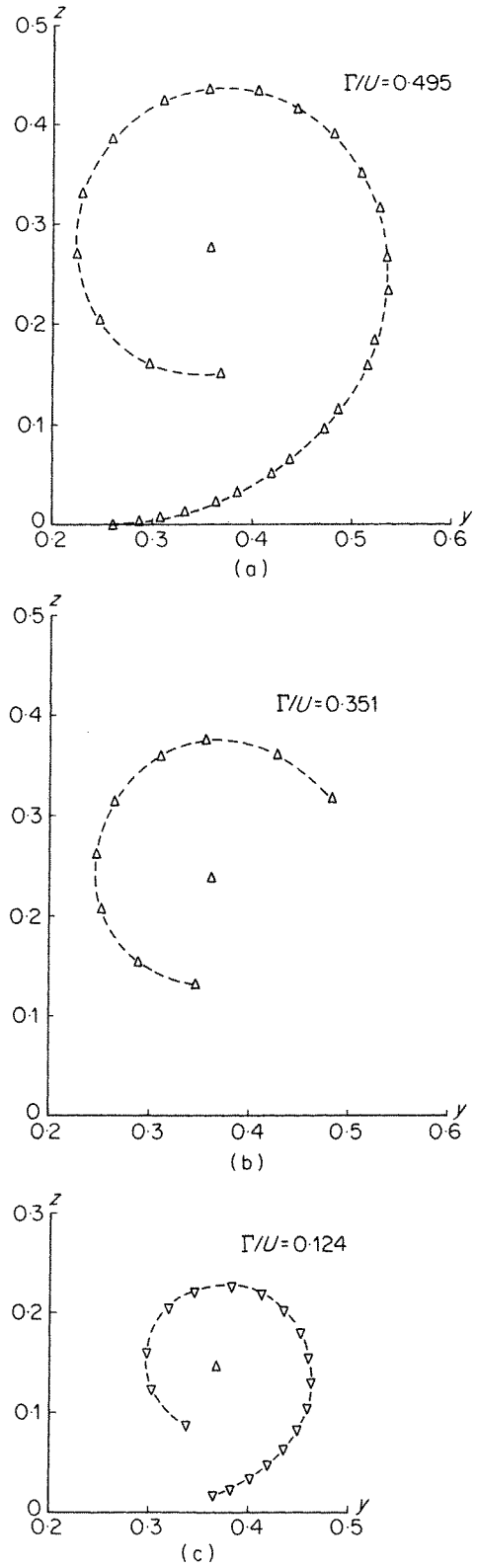


Figure 15. Lenticular wing—sheet shapes, $x = 3{\cdot}0$: (a) $\alpha = 0{\cdot}25$; (b) $\alpha = 0{\cdot}2$; (c) $\alpha = 0{\cdot}1$

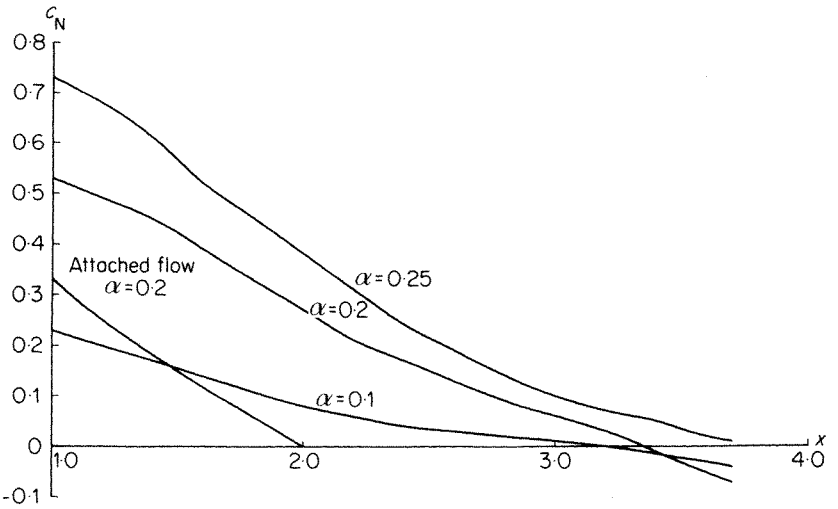


Figure 16. Lenticular wing—local normal force coefficient

The distribution of the local normal force coefficient is shown in Figure 16 for all three incidences, together with the attached flow solution for $\alpha = 0{\cdot}2$. The attached flow theory predicts zero additional lift downstream of the maximum span, at $x = 2{\cdot}0$. Further, the linearized lifting surface theory of R. T. Jones[19] predicts zero vortex lift on sections downstream of the maximum span. This is due to the use of Prandtl's assumption that the vortex sheet shed from the trailing edge of a slender wing remains coplanar in its vicinity. From the present results, for $\alpha = 0{\cdot}2$, we can see that we have additional vortex lift on the forward part of the wing and, for all three incidences, the calculations predict lift on the rear of the wing, where the rolling up of the vorticity has violated the assumption of Prandtl. A similar conclusion was drawn by Fink and Soh[20] who applied their vortex sheet model to a slender wing of rhombic planform.

## 7. CONCLUSIONS

An inviscid multi-vortex model has been developed for the description of vortices shed from the sharp leading edges of slender wings. Results obtained from the method have been shown to give good agreement with a vortex sheet model where comparison is available. Further, the method has widened the class of problems which can be dealt with, namely, those in which more than one coherent vortex structure is present. Results for such problems have been obtained as far downstream as the point where the vortex systems begin to merge.

ACKNOWLEDGEMENTS

The author would like to thank Professor N. Riley, University of East Anglia and Mr. J. H. B. Smith, R.A.E., Farnborough, for their help during the period in which this research was carried out and for their useful comments in the preparation of this paper. The research was supported by the U.K. S.E.R.C. in collaboration with the Aerodynamics Department, R.A.E.

## REFERENCES


1. C. E. Brown and W. H. Michael, 'On slender delta wings with leading-edge separation', *J. Aero. Sci.*, **21,** 690–694 and 706 (1954); [see also *NACA TN 3430* (1955)].
2. J. H. B. Smith, 'A theory of the separated flow from the curved leading edges of a slender wing', *ARC R & M No. 3116* (1957).
3. J. H. B. Smith, 'Improved calculations of leading-edge separation from slender delta wings', *Proc. Roy. Soc.*, **A306,** 67–90 (1968); [see also *RAE Tech. Rep. 66070* (ARC 27897) (1966)].
4. R. W. Clark, 'Non-conical flow past slender wings with leading-edge vortex sheets', *ARC R & M No. 3814* (1978).
5. A. M. Sacks, R. E. Lundberg and C. W. Hanson, 'A theoretical investigation of the aerodynamics of slender wing-body combinations exhibiting leading-edge separation', *NASA CR-719* (1967).
6. D. W. Moore, 'A numerical study of the roll-up of a finite vortex sheet', *J. Fluid Mech.*, **63,** 225–235 (1974).
7. R. R. Clements and D. J. Maull, 'A representation of sheets of vorticity by discrete vortices', *Prog. Aerospace Sci.* **16,** 129–146 (1975).
8. M. S. Longuet-Higgins, 'Oscillating flow over steep sand ripples', *J. Fluid Mech.*, **107,** 1–35 (1981).
9. J. M. R. Graham, 'The forces on sharp-edged cylinders in oscillatory flow at low Keulegan–Carpenter numbers', *J. Fluid Mech.*, **97,** 331–346 (1980); [see also 'Vortex shedding from sharp edges', *Imperial College Aero Report 77–06* (1977)].
10. P. T. Fink and W. K. Soh, 'A new approach to roll-up calculations of vortex sheets', *Proc. Roy. Soc.*, **A362,** 195–209 (1978).
11. D. W. Moore, 'On the point vortex method', unpublished report (1980).
12. H. Portnoy, private communication (1981).
13. G. N. Ward, *Linearized Theory of Steady High-speed Flow*, CUP (1955).
14. J. H. B. Smith, private communication (1979).
15. A. J. Peace, 'A contribution to the theory of aerodynamic vortex flows', *Ph.D. thesis*, University of East Anglia (in preparation).
16. J. D. Lambert, *Computational Methods in Ordinary Differential Equations*, Wiley (1973).
17. S. P. Fiddes, private communication (1980).
18. D. W. Moore, 'The stability of an evolving two-dimensional vortex sheet', *Mathematika*, **23,** 35–44 (1976).
19. R. T. Jones, 'Properties of low-aspect-ratio pointed wings at speeds below and above the speed of sound', *NACA rep. No. 835* (1946).
20. P. T. Fink and W. K. Soh, 'On an anomalous result in linearized slender lifting surface theory', *Univ. New S. Wales report NAV/ARCH 74/6* (1974).